Journal of Materials Chemistry B

Accepted Manuscript

This article can be cited before page numbers have been issued, to do this please use: J. Xu, F. Zeng, H. Wu and S. Wu, *J. Mater. Chem. B*, 2015, DOI: 10.1039/C5TB00522A.

ROYAL SOCIETY OF CHEMISTRY

www.rsc.org/materialsB

View Article Online
DOI: 10.1039/C5TB00522A

Journal Name

RSCPublishing

ARTICLE

A Mitochondria-targeted and NO-based Anticancer Nanosystem with Enhanced Photo-controllability and Low Dark-toxicity

Cite this: DOI: 10.1039/x0xx00000x

Received 00th January 2012,
Accepted 00th January 2012

DOI: 10.1039/x0xx00000x

www.rsc.org/

Jiangsheng Xu, Fang Zeng*, Hao Wu, Shuizhu Wu*

Compared to the generation of singlet oxygen in photodynamic therapy, photo-generation of nitric oxide (NO) would not be limited by the concentration of molecular oxygen. However, the therapeutic applications of exogenous nitric oxide are usually limited by its short half-life and its vulnerability to many biological substances, thus straightforward and precise control of NO delivery may be critical to its therapeutic effects. Herein, we demonstrate a mitochondria-targeted and photoactive NO-releasing system as an anticancer drug. Fabricated by covalently incorporating a photo-responsive NO-donor and a mitochondria targeting ligand onto carbon dot, this nanosystem exhibits a multi-functional nature which combines mitochondria-targeting, photocontrollable NO-releasing and cell imaging. Upon cellular internalization, the nanosystem could target mitochondria effectively. Furthermore, the system displays little dark toxicity under physilogical temperature; but upon light irradiation, it could release NO, efficiently damage the mitochondria and consequently cause prominent apoptosis of cancer cells. Moreover, evaluated by using MTT assay, this nanosystem shows high cytotoxicity towards two cancer cell lines. These observations provide new insights for exploiting NO in disease therapy.

Introduction

Nitric oxide (NO), one of the most appealing and studied molecules in the fascinating realm of biomedical sciences, plays important roles in various physiological as well as pathological processes, such as tumor growth and suppression.[1-3] Endogenous NO mediates multiple processes in various physiological systems including cardiovascular system, immune system, and the central and peripheral nervous system. On the other hand, a number of potential therapeutic applications of exogenous NO delivery in cardiovascular diseases, respiratory diseases, cancer treatment, antimicrobial therapy, wound healing, and functional biomedical devices have so far been proposed and explored.[4-7] In particular, human solid tumors contain hypoxic regions that have considerably lower oxygen tension than normal tissues.[6,8] This imparts resistance to radiotherapy and anticancer chemotherapy. For instance, photodynamic therapy involves three main components: a photosensitizer (PS), molecular oxygen and light,[9,10] which means the lack of molecular oxygen in tumor tissue or cells would reduce the efficacy of the photodynamic treatment. Compared to singlet oxygen generation, photo-generation of NO involves a neat photochemical reaction without the dependence on oxygen.

In response to the need for NO delivery, researchers have paid great attention to the development of NO donors.[11,12] For example, to improve NO's pharmacological potential, Schoenfisch et al. have fabricated a number of NO-releasing scaffolds featuring enhanced NO storage and some other advantageous properties;[13-15] Ford and coworkers used several metal complexes as the photochemical NO donor in cancer treatment; and this photochemical strategy allows for good control of the timing and dosage for the NO delivery.[16-18] On the other hand, Sortino's group developed a variety of light-controlled NO delivering molecular assemblies (such as nanostructured films, polymers, nanoparticles and etc.) through different approaches,[19-24] and these assemblies exhibit promising potential in NO-involved therapeutic applications. However, severe limitations do exist for NO-involved therapeutic applications. This ephemeral species has a very short lifetime and exhibits high reactivity with many biological substances, which makes NO-based therapies highly site, concentration and dosage dependent.[25-29] And the solutions, which enable us to precisely determine where, when, and to what extent a process is started or stopped, are highly desirable.

Among the possible solutions able to harness the release of therapeutics, the use of light is definitely one of the most elegant ones.[22] Light has an easy manipulation with an exquisite spatiotemporal control in terms of intensity, wavelength, duration and location. It can be generated and manipulated with well-established techniques and also harmless if applied correctly.

On the other hand, the mitochondria are energy factories of the cell, playing important roles in energy metabolism of

ARTICLE View Article Online
DOI: 10.1039/C5TB00522A Journal Name

various biochemical processes. They exert a variety of important cellular functions including the production of the largest part of cellular ATP needed for endergonic processes.[30,31] They are also the central regulators of cellular metabolism and the executioners of programmed cell death (apoptosis).[25,32-35] Thus, mitochondria-targeting ligands have been used as effective vectors for some therapeutic drugs that affect mitochondrion function, the apoptotic pathway, or other signal transduction factors localized in mitochondria. Some ligands such as phosphonium derivatives have been employed by Murphy, Chang and others to target mitochondria as these lipophilic cations selectively accumulate in mitochondria due to proton gradient considerations.[36-39]

It also has been found that many of the regulatory tasks undertaken by NO in the cell are associated with mitochondria.[40,41] Mitochondrion is the main area where endogenous NO is synthesized by inducible NO synthase (iNOS) in mammalian cells and plays a critical role in regulating cell functions. Increasing amount of evidences suggests that small amounts of NO stimulate mitochondrial biogenesis and boost the supply of oxygen and respiratory substrates to mitochondria. In contrast, high level of NO endogenously produced by inducible NO synthase (iNOS) block mitochondrial respiration, and can be cytotoxic.[42-44] NO is cytotoxic partly because mitochondrial NO can inactivate the respiratory chain enzymes by binding to the heme group of cytochrome c oxidase or by controlling mitochondrial pH, and partly because NO can be further oxidized into $ONOO^-$, N_2O_3, NO_2^-, and NO_3^- by excess reactive oxygen species and induces nitrosative damage to proteins, ultimately stimulates the mitochondrial pathway of apoptosis.[45] Despite of the fact that the mitochondria maintain homeostasis in the cell by interacting with NO and other reactive nitrogen species (RNS) and there is a growing consensus of the vital role mitochondria play in medicine (e.g. mitochondrion has recently emerged as a promising therapeutic target in cancer treatment),[46,47] the investigation on the interaction of NO-releasing pharmacological agents with mitochondria is too often disregarded, and to date only a few reseaches involving both the mitochondria-targeting and NO-releasing have been reported.[48-51] Nakagawa, Miyata and coworkers, for the first time, demonstrated effective NO-releasing systems for time-controlled, mitochondria-specific NO treatment, which were synthesized by linking a NO donor, a mitochondria-targeted moiety and a fluorophore. And the intracellular localization of these molecular NO-releasing systems could be clearly observed under confocal microscope due to their fluorescent nature.[49,50] On the other hand, our group has developed a mitochondria targeting and NO-releasing nanosystem and used it as a pro-apoptosis agent in cancer theraphy.[51] However, we could not precisely control the release of NO by using light, since the nanosystem was also heat-responsive and slowly released NO at 37 °C in the dark.

Recently, carbon dots (Cdots), as a new class of fluorescent nanoparticles, have attracted growing interest due to their alluring optical and biological properties, such as water solubility, biocompatibility and excellent cell membrane permeability, tunable surface functionalities and good photostability.[52-57] More importantly, their small size (less than 10 nm) makes them very suitable as the carriers for subcellular organelles targeting; and their photoluminescence allows for visualization of the intracellular trafficking of the drug delivery system.

To gain enhanced control over the NO release, we herein prepared a new mitochondria-targeting and photoactive NO-releasing system as an anticancer drug, as shown in Scheme 1. For this system, a triphenylphosphonium moiety which was used as a mitochondria-targeting ligand and a photo-responsive NO donor 4-nitro-3-(trifluoromethyl) aniline derivative were conjugated onto the carbon dots. Multi-functionality (including mitochondria-targeting, efficient light-triggered NO-releasing and cell imaging) was achieved for the nanosystem. In this study, we evaluated the action of the nanosystem on two cancer cell lines; and our results indicate that, the mitochondria-targeted and NO-releasing system can cause high toxic effect towards the cancer cells by specifically damaging their mitochondria upon light irradiation. Our study demonstrates that the combination of mitochondria-targeting and highly controlled NO-releasing can enhance the system's pro-apoptosis action, thereby providing new insights for exploiting NO in cancer therapy with the ultimate goal of maximizing the therapeutic action while minimizing side effects.

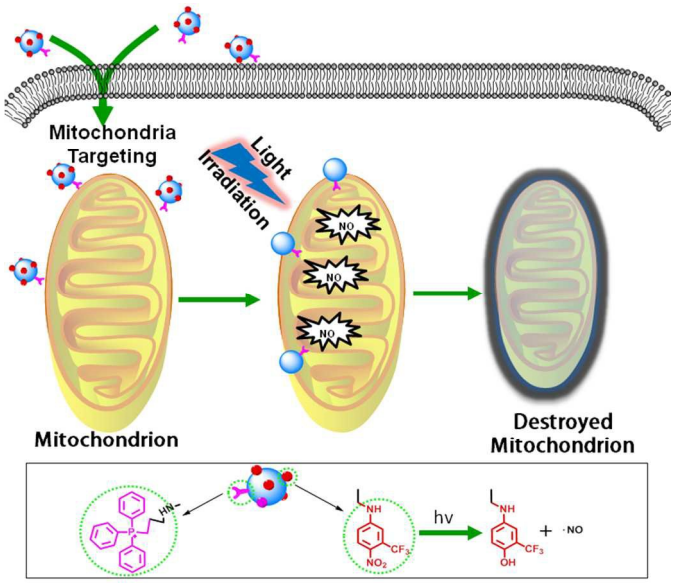

Scheme 1. Schematic illustration for the action of the Cdot-based multi-functional system on the mitochondrion of a cancer cell.

Experimental

Materials.

Citric acid, triphenylphosphine, ethylenediamine, 3-bromopropionic acid, 3-bromopropylamine hydrobromide, 5-chloro-2-nitrobenzotrifluoride, 4-nitro-3-(trifluoromethyl)aniline, 1,3-propanediamine 1,4-dibromobutane, N-(1-naphythyl)-ethylenediamine dihydrochloride (NEED) and sulfanilamide (SULF) were supplied by Aladdin Industrial Inc. 1-Ethyl-3-(3-dimethylaminopropyl) carbodiimide hydrochloride (EDC-HCl), sulfo-N-hydroxysuccinimide (sulfo-NHS) and rhodamine 123 (RhB123) were purchased from Sigma-Aldrich. The culture medium RPMI1640 and the bovine serum albumin (BSA) were obtained from Invitrogen. Triethylamine (TEA), N,N-dimethylformamide (DMF) and dimethyl sulfoxide (DMSO) were distilled before use. JC-1 (5,5',6,6'-tetrachloro-1,1',3,3'-

Journal Name

View Article Online
DOI: 10.1039/C5TB00522A ARTICLE

tetrethyl benzimidazolylcarbocyanine iodide), LysoTracker Red and annexin V-FITC kit were purchased from the Beyotime Institute of Biotechnology. All other chemicals used were of analytical reagent grade. The water used in this study was the triple-distilled water which was further treated by ion exchange columns and then by a Milli-Q water purification system.

Synthesis of (3-Carboxyethyl)triphenylphosphonium Bromide (TPP-COOH). A solution of 3-bromopropionic acid (1.53 g, 10mmol) and triphenylphosphine (2.62 g, 10 mmol) in CH_3CN (25 mL) was stirred at reflux for 15 h. Then the solvent was removed, and the resulting white solid was purified by silica gel flash chromatography ($MeOH:CH_2Cl_2$ =10:1) to produce the white solid (2.6 g, 64% yield). ^1H NMR (400 MHz, $CDCl_3$, δ) 7.86 – 7.75 (m, 15H), 3.64 (m, 2H), 3.76 (t, J = 7.2 Hz, 2H), 3.08 (m, 2H). ESI-MS m/z $[M-Br]^+$ = 334.14.

Synthesis of (3-aminopropyl)triphenylphosphonium Bromide (TPP-NH_2). An amino-containing triphenylphosphonium (TPP-NH2) was synthesized as described below: briefly, a solution of 3-bromopropylamine hydrobromide (2.19 g, 10 mmol) and triphenylphosphine (2.62 g, 10 mmol) in CH_3CN (25 mL) was stirred at reflux for 15 h. The resultant precipitate was collected by filtration and then dissolved in H_2O and treated with saturated aqueous K_2CO_3 until the pH reached 11. The product was extracted into 2 vol of CH_2Cl_2, dried (by $MgSO_4$), filtered; then the solvent was removed, and the resulting white solid was purified by silica gel flash chromatography (MeOH: CH_2Cl_2 =10:1) to produce the white solid (1.2 g, 24% yield). ^1H NMR (400 MHz, MeOD, δ) 7.96 – 7.75 (m, 15H), 3.64 (m, 2H), 3.26 – 3.17 (t, J = 7.2 Hz, 2H), 2.05 (m, 2H). ESI-MS m/z $[M-Br]^+$ = 319.9.

Synthesis of N-(3-aminopropyl)-4-nitro-3-(trifluoromethyl) aniline (NF-NH_2). 5-chloro-2-nitrobenzotrifluoride (225 mg, 1.0mmol) and 1,3-propanediamine (158 mg, 2.0 mmol) were refluxed in 25 mL MeCN for three days. The obtained solution was concentrated under reduced pressure and purified by column chromatography (CH_2Cl_2:MeOH, 2:1) to give N-(3-aminopropyl)-4-nitro-3-(trifluoromethyl)aniline (yield 60%) as a yellow solid. ^1H NMR (600 MHz, $CDCl_3$, δ) 8.01 (t, 1H), 6.93 – 6.79 (m, 1H), 6.63 (d, 1H), 6.51 – 6.34 (m, 1H), 3.37 – 3.25 (m, 2H), 2.93 (d, 2H), 1.85 – 1.77 (m, 2H). ESI-MS m/z $[M+H]^+$ = 264.18.

Synthesis of N-(4-bromobutyl)-4-nitro-3-(trifluoromethyl)aniline (Br-NF). 4-Nitro-3-(trifluoromethyl)aniline (206 mg, 1.0 mmol) and 1,4-dibromobutane (928mg, 2.0 mmol) were refluxed in 25 mL MeCN for three days. The resultant solution was concentrated under reduced pressure and purified by column chromatography (CH_2Cl_2: MeOH, 50:1) to give N-(4-bromobutyl)-4-nitro-3-(trifluoromethyl)aniline (yield 70%) as a yellow solid. ^1H NMR (400 MHz, $CDCl_3$, δ) 8.09 (d, 1H), 6.84 (s, 1H), 6.59 (d, 1H), 3.44 (t, 4H), 2.18 – 2.06 (m, 4H).

Synthesis of mitochondrial-targeting and NO-releasing Molecule (MitoNF). TPP-COOH (167 mg, 0.5 mmol) was treated with EDC • HCl (115 mg, 0.6 mmol) in 10 mL CH_2Cl_2 with stirring at room temperature for 30 min before being added to the solution of NF-NH_2 (130 mg, 0.5 mmol) in THF (10 mL) and 35 μL TEA. The mixture was stirred at room temperature overnight, then the solvent was removed, and the resulting yellow solid was purified by silica gel flash chromatography ($MeOH:CH_2Cl_2$ =10:1) to produce the yellow solid MitoNF. ^1H NMR (400 MHz, $CDCl_3$, δ) 8.86 (t, 1H), 7.87 – 7.69 (m, 15H), 7.14 (t, 1H), 6.98 (s, 1H), 6.77 (d, 1H), 3.60 – 3.51 (m, 2H), 3.31 (d, 4H), 1.88 – 1.78 (m, 2H). ESI-MS m/z $[M-Br]^+$ = 579.38.

Synthesis of Cdots with targeting ligand (MitoCdot). Cdots were prepared according to our previously reported procedure.[51] Cdots (200 mg) was treated with EDC • HCl (345 mg, 1.8 mmol) and sulfo-NHS (345 mg, 1.59 mmol) in 25.0 mL DMSO with stirring at room temperature for 1 h before being added to the solution of (3-aminopropyl)triphenylphosphonium bromide (TPP-NH2) (120 mg, 0.3 mmol) in 10.0 mL DMSO and 150 μL of TEA. The mixture was stirred at room temperature for another 48 h. The resultant solid was precipitated out by addition of sufficient amount of diethyl ether/acetone (7:3) and washed repeatedly with methanol and ethanol respectively. Thereafter, the red-brown solid was dissolved in purified water and dialyzed against purified water using a dialysis tubing (molecular weight cut-off 100 Da) for 48 h. The solid was collected by freeze-drying.

Synthesis of mitochondrial-targeting and NO-releasing nanosystem (MitoCdot-NF). MitoCdot (100 mg), EDC • HCl (192 mg, 1.0 mmol) and sulfo-NHS (212 mg, 1.0 mmol) were dispersed in 10 ml DMSO, and placed into a 50 ml round-bottomed flask under N_2 atmosphere at room temperature. After 1 h of stirring, N-(3-aminopropyl)-4-nitro-3-(trifluoromethyl) aniline NF-NH_2 (130 mg, 0.5 mmol) and TEA (100 μL) were added to the dispersion. The mixture was stirred at room temperature for 24 h in dark. The resultant solid was precipitated out by addition of sufficient amount of diethyl ether/acetone (7:3) and washed repeatedly with methanol and ethanol respectively, and then dialyzed against purified water for 4 days in dark. The solid was collected by freeze-drying to give 78 mg of MitoCdot-NF.

Synthesis of NO-releasing nanosystem without targeting ligand (Cdot-NF). The control, Cdot-NF, was prepared with a similar procedure as that of MitoCdot-NF by using pristine Cdots instead of MitoCdot.

Characterization. ^1H NMR spectra were recorded on a Bruker Avance 400 MHz NMR spectrometer. UV-vis spectra were recorded on a Hitachi U-3010 UV-vis spectrophotometer. Fluorescence spectra were recorded on a Hitachi F-4600 fluorescence spectrophotometer. Confocal Laser Scanning Microscopy (CLSM) images were collected using a Leica TCS-SP5 confocal microscope. Atomic-force microscopy (AFM) was performed on a DI Veeko Multimode V atomic force microscope operated in the tapping mode. High-resolution transmission electron microscopy (HR-TEM) was performed on a JEM-2100HR electron microscope. Dynamic light scattering measurement was carried out on a Malvern Nanosizer. Flow

View Article Online
DOI: 10.1039/C5TB00522A
Journal Name

cytometry were performed on a Beckman Coulter Epics XL flow cytometer.

Photo-triggered variation in absorption spectrum of MitoCdot-NF. The variation in absorption spectrum for nanosystem upon light irradiation at different time periods were determined using UV-vis spectra method, MitoCdot-NF samples were incubated at a simulated physiological condition (PBS, pH 7.4) at 37 °C in dark or under a 12 W LED lamp (spectral peak position at 400 nm) with light intensity at 10 mW/cm^2. The absorbance spectra were recorded.

NO Release Assay: The production of NO by the nanosystem was determined using Griess assay. MitoCdot-NF samples were incubated at a simulated physiological condition (PBS, pH 7.4) at 37 °C in dark or under light irradiation, and the release of NO from nanosystem was monitored as nitrite (NO_2^-) formation by using the Griess reaction. Typically, 1mL solution of nanosystem was immersed in a quartz cuvette containing Griess solution (SULF 0.1 mol L^{-1}, NEED 0.1 mol L^{-1}, HCl 4.0 mol L^{-1}). The absorbance at 550 nm, which provides a quantitative measurement of NO released to the solution after its conversion to NO_2^-, was kinetically monitored at 37 °C. The relationship of absorbance and concentrations of nitrite was constructed by drawing a standard curve from known concentrations of $NaNO_2$.

Cell Culture. Two cancer cell lines, HeLa (human cervical cancer cell) and HepG2 (human liver carcinoma cell) were incubated in RPMI 1640 medium supplemented with 10% fetal bovine serum (FBS) at 37 °C with 5% CO2. The cells were regularly subcultured to maintain them in a logarithmic phase of growth.

Co-localization Imaging. One day before imaging, cells were passaged and plated on polylysine-coated cell culture glass slides inside 30-mm glass culture dishes and allowed to grow to 50-70% confluence. Afterwards, cells (on glass slides) were washed with RPMI1640, and re-incubated in RPMI1640 medium containing the C-dot-based sample (0.30 mg/mL) and a fluorescent dye (2 μM rhodamine 123, 1 μg/mL JC-1 or 500 μM LysoTracker Red) at 37 °C under 5 % CO_2 for a certain period of time. Afterwards, the culture dishes were washed with PBS, and the cells (on glass slides) were taken out and washed with PBS for three times and then placed on a Leica TCS SP5 laser confocal scanning microscope for imaging (using a 100×1.4 NA objective). The laser excitation wavelength for the samples was 405 nm and their fluorescent signals were collected from 415 to 510 nm (blue channel). Rhodamine 123 was excited at 488 nm, and its emission was collected from 515 to 550 nm (green). Lyso Tracker Red was excited at 543 nm, and its emission was collected from 580 to 630 nm (red). All image acquisitions and analyses were performed using Leica LAS AF software. The intensity of the laser beam and the photodetector sensitivity were kept constant in order to compare the relative fluorescence intensities among experiments.

Determination of Change in Mitochondrial Membrane Potential. Two different methods were employed to detect mitochondrial membrane potential changes using the fluorescent probe JC-1.

For flow cytometry, cells were treated for 4 h with the nanosystem (during which the cells were also subject to 15 or 30 min of light irradiation) in 6-well plates and were then washed three times with warm PBS. The cells were then detached with trypsin –EDTA solution. Collected cells were incubated for 30 min with 1 μg/mL of JC-1 in culture medium at 37 °C in the dark. Stained cells were collected in 37 °C PBS/2% BSA and washed twice by centrifugation. Finally, cells were resuspended in 0.3 mL of PBS with 2% BSA and used for data acquisition. A Beckman Coulter Epics XL equipped with a 488 nm argon laser was used in the study. After the flow cytometer was set for green (FL-1) and red (FL-2) fluorescence, the data were collected and analyzed with Beckman Coulter EXPO 32 software.

For imaging (mitochondria damage), cells were passaged and plated on polylysine-coated cell culture glass slides inside 30-mm glass culture dishes and allowed to grow to 50-70% confluence. Fresh staining solution (1 μg/mL) was prepared immediately before use by diluting a 100× stock solution of JC-1 in warm (37 °C) culture medium supplemented with 10% FBS. Cells treated with NO-releasing nanosystems for 4 hours (during which the cells were also subject to 30 min of light irradiation) were incubated with JC-1 for 30 min in a 37 °C CO_2 incubator. Cells were then washed twice with warm PBS and examined immediately under a Leica TCS-SP2 confocal microscope. The JC-1 was excited at 488 nm, and light emissions were collected between 515 and 545 nm (green) and at 570-600 nm (red). All image acquisitions and analyses were performed using Leica LAS AF software. The intensity of the laser beam and the photodetector sensitivity were kept constant in order to compare the relative fluorescence intensities between experiments.

Cell Viability Assay. The viability of HeLa and HepG2 cells treated by Br-NF, Mito-NF, MitoCdot-NF, MitoCdot or Cdot-NF subject to light irradiation were assessed by MTT assay. The cells were cultured in RPMI 1640 medium supplemented with 10% FBS. The cells were seeded in 96-well plates at the cell population of ca. 5000 cells/well. After 24 h of incubation in 96-well plates at 37 °C, cells were washed with prewarmed PBS buffer, then the PBS was replaced with fresh medium containing MitoCdot, MitoCdot-NF or Cdot-NF (corresponding to 0 ~ 100 μM of NF moiety) and the samples were incubated for 4 h, and then the cells were exposed to 400 nm light (using a 12 W LED lamp with light intensity at 10 mW/cm^2) for 30 min. The samples were then incubated for another 19.5 h. Thereafter, the wells were washed with PBS buffer and incubated for another 4 h with RPMI 1640 medium containing 0.5 mg/mL MTT. After discarding the culture medium, 150 μL of DMSO was added to dissolve the precipitates and the absorbance was read with a Thermo MK3 ELISA reader at 570 nm. As for cell viability without light illumination (dark

Journal Name

View Article Online
DOI: 10.1039/C5TB00522A ARTICLE

cytotoxicity), similar procedures were adopted only without the light illumination. As for all the assays, three independent experiments were performed for each concentration, and for each independent experiment, the assays were performed in eight replicates. And the statistical mean and standard deviation were used to estimate the cell viability.

Statistical Analysis. All data are reported as mean ± SD from three independent experiments, each performed in eight replicates; differences between groups were assessed by one-way ANOVA with Tukey's post hoc test.

Results and discussion

Preparation of mitochondrial-targeting and NO-releasing systems.

In this study, a 4-nitro-3-(trifluoromethyl) aniline derivative was synthesized as the nitric oxide donor; and a triphenylphosphonium (TPP) derivative was used as the ligand to target mitochondria. For comparison, we prepared two molecular NO-releasing systems and two Cdot-based NO-releasing systems (Br-NF, Mito-NF, Cdot-NF and MitoCdot-NF, their structures are shown in Figure 1A and the synthesis routes are shown in Scheme S1). Among them, Br-NF and Cdot-NF, which have no triphenylphosphonium in their structures, were used as control systems to verify the mitochondria targeting capability of Mito-NF and MitoCdot-NF. The structures of the intermediates and final products were well confirmed and characterized (Figures S1- S11 in the Supplementary Information). The content of carboxyl groups on as-prepared Cdot surface was determined as 318.87 μM/g carbon dots (or about 12 carboxyl groups per Cdot), as described in Figure S8 and S9. And the content for the targeting ligand (TPP) and the NO donor (NF) on MitoCdot-NF were determined as 9.96 mg/g (39.8 μM/g) and 39.12 mg/g (146.2 μM/g), respectively, as described in Figure S7, S10 and S11. The high resolution transmission electronic microscope (HR-TEM), dynamic light scattering (DLS) and atomic force microscope (AFM) analysis results for MitoCdot-NF are given in Figure 1B, 1C and 1D. The average diameter for MitoCdot-NF determined from dynamic light scattering measurement is 4.5 nm (Figure 1 C), and the nanoparticles generally exhibit spherical shape (Figure 1B and 1D).

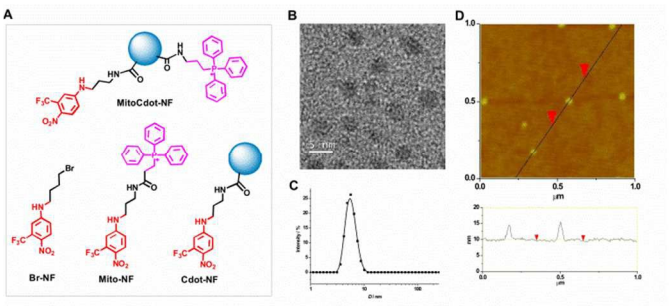

Figure 1. Structures of four NO-releasing systems (A). The HR-TEM (B), DLS (C) and AFM (D) analysis results for Mito-Cdot-NF. The lower panel of (D) gives the height profile along the line in the topographic image in the upper panel.

The spectral properties for some NO-releasing systems are given in Figure 2. It can be seen from Figure 2(A), with the NO donor (4-nitro-3-(trifluoromethyl)aniline, NF) in their structure, both the nanosystem MitoCdot-NF and the molecular Mito-NF exhibit an absorption bond at 402 nm. On the other hand, MitoCdot-NF displays a strong emission band at 460 nm when excited at 405 nm, and an extremely weak emission when excited at 488 nm (Figure 2B). This is important for subsequent cell imaging studies because the emission behavior of the Cdot allows us to trace the cell uptake of the nanosystem, but does not interfere with other imaging experiments.

Light induced NO release.

The light-induced spectrum changes for the NO-releasing systems are demonstrated in Figure 2C, 2D and in Figure S12. One can see from the figures that, with the increasing irradiation time, the absorbance for MitoCdot-NF or Mito-NF decreases, this is due to the photo-bleaching of NO donor (NF), which is accompanied by the release of NO.[20,21] In contrast, the NO-releasing systems exhibit almost no decrease in absorbance in the absence of light irradiation (Figure 2D, Figure S13). In addition, the Griess assay[58] was adopted to confirm the generation of NO by the nanosystem upon photo-irradiation (Figure S14-S16). First, a standard curve (Figure S14) for the assay was constructed using $NaNO_2$ (the reaction product of NO and Griess agent) of known concentrations. The absorption spectra for MitoCdot-NF treated by Griess agent over different periods of time under irradiation in pH 7.4 PBS buffer at 37°C are given in Figure S15; and the concentrations of NO released from the sample over time by Griess assay with or without irradiation are presented in Figure S16. It is clear that without the light irradiation, there is almost no nitric oxide released from the nanosystem, while continuous light exposure results in NO production, as evidenced by the enhancement of the absorption at 540 nm. This indicates that the release of NO for the systems at 37 °C is strictly dependent on the external light inputs, and the systems do not exhibit heat response.

ARTICLE View Article Online
DOI: 10.1039/C5TB00522A Journal Name

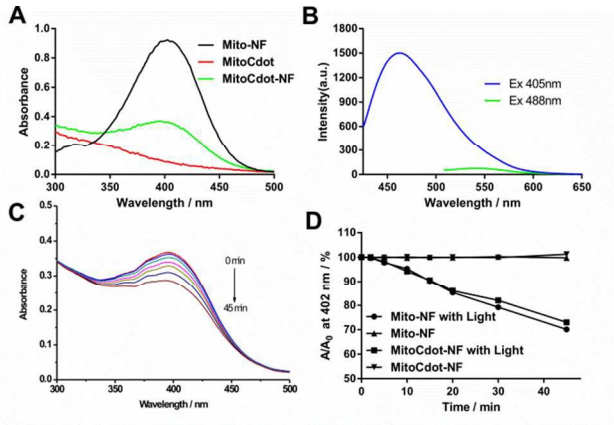

Figure 2. (A) Absorption spectra for three TPP-containing systems. Among them, MitoCdot is a control sample which was prepared by linking triphenylphosphonium onto carbon dot; (B) Emission spectra for MitoCdot-NF excited at 405 nm or 488 nm, respectively; (C): Absorption spectra variation for MitoCdot-NF over different time periods under 400 nm light irradiation, the arrows indicate the spectral evolution with irradiation time from 0 to 45 min; (D): Absorbance values at 402 nm for Mito-NF and MitoCdot-NF plotted against irradiation time in pH=7.4 buffers at 37 °C. In (C) and (D), the concentration for MitoCdot-NF is 133 μg/mL, equivalent to 19.5 μM of NF.

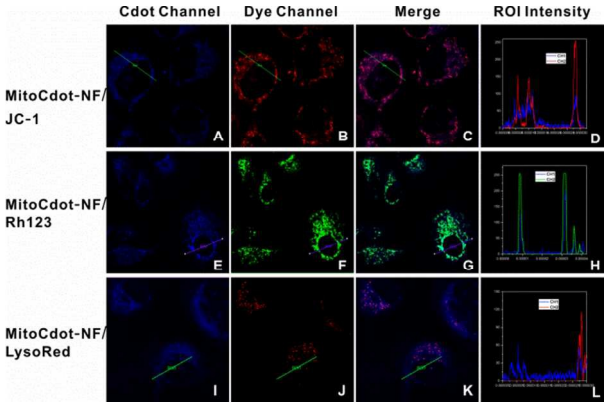

Figure 3. Confocal microscopic images for HeLa cells respectively co-stained with MitoCdot-NF/JC-1 (A – C), MitoCdot-NF/rhodamine 123 (E – G) or MitoCdot-NF/LysoTracker Red (I –K). (D), (H) and (L): Intensity profile of ROIs across the cells. For Figure 3B, signals only from red-channel were collected. Concentration of MitoCdot-NF: 300 μg/mL; JC-1: 1 μg/mL; Rh123: 2 μM; LysoRed: 500 μM.

Mitochondria Targeting of the Nanosystem.

To verify the triphenylphosphonium (TPP)-modified nanosystem can target and specifically stain the mitochondria, two mitochondria-specific staining dyes, rhodamine 123 (Rh123) and JC-1, were employed to co-stain HeLa cells with MitoCdot-NF. Figure 3 (A, B, E and F) shows the confocal fluorescence images for the cells co-stained by MitoCdot-NF and rhodamine 123 (or JC-1). The Cdots show blue fluorescence; while Rh123 shows green fluorescence, and the J-aggregates of JC-1 dye exhibit red fluorescence in cells. The merged images (Figure 3C and 3G) indicate effective overlap for the Rh123/MitoCdot-NF pair or JC-1/MitoCdot-NF pair. These fluorescence images all indicate the selective accumulation of the nanosystem in mitochondria. In addition, as shown in Figures 3D and 3H, the intensity profiles of linear regions of interest (ROIs) also prove that the nanosystem exhibits greater overlap with Rh123 or JC-1. These results suggest that, with the targeting ligand on its surface, MitoCdot-NF specifically stains the mitochondrial region in live cells.

On the other hand, the use of nanosystems to target mitochondria is often limited by the fact that nanosystems is taken up by the endocytic pathway, and in this pathway endosomes/lysosomes serve as the barrier to mitochondrial trafficking. Thus, to rule out the possibility that the current nanosystems mainly distribute in endosomes/lysosomes upon cell uptake, we performed a co-localization experiment using the MitoCdot-NF and a lysosome marker LysoTracker Red, and the results are also presented in Figure 3 (I-K). It is clear that there is a poor match between the intracellular blue fluorescence (from MitoCdot-NF) and the red fluorescence (from the lysosome marker), suggesting the good lysosomal escape ability of the nanosystem.

Mitochondria damage induced by NO.

The exact molecular mechanism of cell apoptosis is not completely clear, but it appears that a variety of key events are focused on mitochondria;[59] and loss of mitochondrial membrane potential ($\Delta\Psi$) is the one of these events.[60] The damaging of mitochondria will lead to the depolarization of mitochondria with a drop in the membrane potential.[61] In this study, a membrane-permeable JC-1 dye was used to monitor mitochondrial status upon NO treatment. The loss of mitochondrial membrane potential ($\Delta\Psi$, a hallmark of cytochrome c translocation and the start of the apoptotic process) is an important indicator to evaluate the dysfunction of mitochondria, since the damaging of mitochondria will lead to the depolarization of mitochondria with a drop in the membrane potential.[62] The JC-1 dye undergoes a reversible change in fluorescence emission, cells with high mitochondrial membrane potential promote the formation of dye aggregates, which fluoresce red; cells with low potential will contain monomeric JC-1 and fluoresce green. Therefore, the red/green ratio can help to identify the status of mitochondria and cells; and we could distinguish live cells from damaged ones following the NO treatment by recording the fluorescence change of JC-1 using confocal microscopy and flow cytometry.

Journal Name

View Article Online
DOI: 10.1039/C5TB00522A ARTICLE

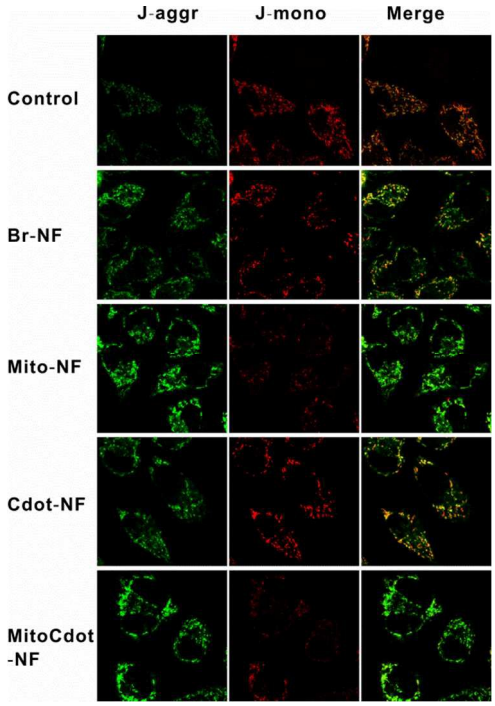

Figure 4. Confocal microscopic images for HeLa cells stained with 1 μg/mL JC-1. Cells were first cultured in 35 mm dishes and incubated respectively with different NO donors (all equivalent to 50 μM of NF, or 342 μg/mL of MitoCdot-NF or 339 μg/mL of Cdot-NF) for 4 h and then exposed to light (using a 400 nm 12 W LED lamp with light intensity at 10 mW/cm^2) for 30 min, and then stained with 1 μg/mL JC-1. The cells without being treated with any of the NO donors were used as the control.

Figure 4 shows the representative results of JC-1 assays for HeLa cells as a result of nitric oxide treatment. Confocal microscopy reveals that in untreated HeLa cells, well-polarized mitochondria are marked by both punctate red and green fluorescent staining. However, treatment with different forms of NO donors (Br-NF, Mito-NF, Cdot-NF, and MitoCdot-NF) respectively followed by light irradiation results in changes in cell staining: the red fluorescence regions gradually decrease, while green fluorescence intensity in the cytoplasm increases. It is noteworthy that the increase of green fluorescence in the cytoplasm is more pronounced when cells are treated with the mitochondria-targeted systems (Mito-NF and MitoCdot-NF), and a big portion of the red dot-like fluorescent images turn into the diffuse green colors (Figure 4). Observed changes in JC-1's fluorescence suggest the decrease of dye aggregate accumulation in mitochondria and the diffusion of JC-1 molecules into cytosol following the increase in the permeability of the mitochondrial membrane with concomitant collapse of mitochondrial membrane potential. The results strongly suggest that, the incorporation of a mitochondria-targeting ligand onto the photoactive NO-releasing system could significantly enhance its mitochondria damaging capability after light irradiation. On the other hand, the carbon dot-based NO-releasing system with mitochondria targeting ligand on its surface (MitoCdot-NF) can damage the mitochondria as efficiently as the molecular mitochondria-targeting system (Mito-NF).

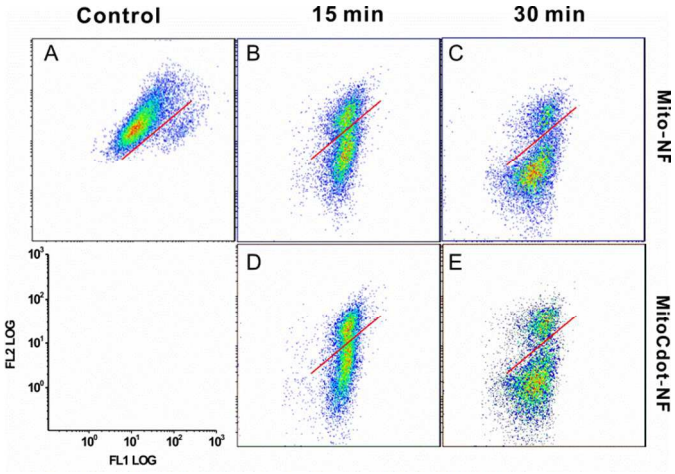

Figure 5. Representative flow cytometric analyses of mitochondrial membrane potential (using JC-1 as indicator) for HeLa cells incubated with Mito-NF (B, C) or Mito-Cdot-NF (D, E) (equivalent to 50 μM of NF, or 342 μg/mL of MitoCdot-NF or 339 μg/mL of Cdot-NF) for 4 hours, and then exposed to light irradiation for 15 min (B, D) and 30 min (C, E) respectively. The shift of JC-1 fluorescence from red (FL2) to green (FL1) indicates a collapse of mitochondrial membrane potential. Red lines separate populations with high (live cells) and low membrane potential (apoptotic cells) according to the untreated HeLa cells (A).

Moreover, we investigated the change in population of cells of different fluorescence following the nitric oxide treatment using flow cytometry with JC-1 as the indicator. Analysis of the cells by flow cytometry reveals a decrease in red fluorescence (FL2 channel) after the treatment with NO donors (NO-releasing systems) and light irradiation (Figure 5). As shown in the figure, without being treated by the NO-releasing system, the cells with high $\Delta\Psi$ predominate in the cell population. However, following the treatment and irradiation, significant increases in the percentage of the cells with low $\Delta\Psi$ are recorded with the increasing time of irradiation, further proving the action of the NO on mitochondria damage. It can also be found in the figure that, compared to molecular NO donor (Mito-NF) (Figure 5 B, C), the Cdot-based system (MitoCdot-NF) induces similarly degree of change in fluorescence upon a certain time of treatment (Figure 5 D, E), suggesting the treatment with the either nano- or molecular-based system can efficiently cause the mitochondrial damage.

To evaluate the efficacy of our NO-releasing systems in cell death, we performed MTT assay for two cancer cell lines (HeLa, HepG2) upon treatment by the targeted (Mito-NF or MitoCdot-NF) system or the non-targeted NO-releasing system (Cdot-NF), and the result is presented in Figure 6. No significant dark toxicity is observed for cells treated with up to 100 μM (concentration of NF, equivalent to 685 μg/mL of MitoCdot-NF or 678 μg/mL of Cdot-NF) of Mito-NF, MitoCdot-NF or Cdot-NF as determined by the MTT assay. This is due to their inability to generate nitric oxide in the dark. After 4 h incubation with the NO-releasing systems followed by 30 min light irradiation, both cell lines treated by mitochondria-targeting systems (MitoCdot-NF, Mito-NF) cause much higher phototoxicity than the system with no mitochondria-targeting ability (Cdot-NF). To rule out the possibility that the reduced viabilities are solely induced by light irradiation or by the enhanced light absorption by the Cdot and/or TPP moieties, we irradiated HeLa cells in the absence of the NO donor, and the results suggest that irradiation alone or the existence of Cdot and/or TPP could not reduce the viability

View Article Online
DOI: 10.1039/C5TB00522A

of the cells (Figure S17 and S18). These results clearly indicate that the preferential localization in the target organelle (mitochondrion) accounts for the enhanced cytotoxicity of the targeted NO-releasing nanosystem.

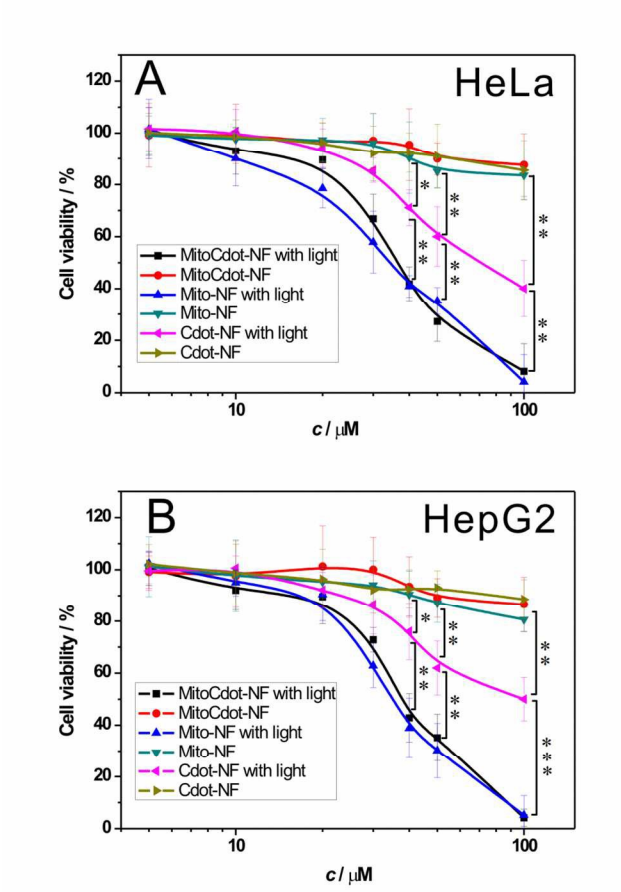

Figure 6. Effect of different NO-releasing systems on viability of two cell lines (HeLa and HepG2). Cell viability was assessed by MTT assay upon 24 h of incubation following the treatment with a NO-releasing system of varied concentrations for 4 hours (with light irradiation for half an hour at intensity or without light irradiation). The horizontal coordinate represents the concentration of NF moiety. Data represent mean ± SD from three independent experiments, each performed in eight replicates. *P<0.05, ** P < 0.01, *** P<0.001.

The therapeutic action of a NO-based drug depends strongly on the concentration and duration of NO delivered. Due to NO's short half-life (seconds) and high activity, effective NO-based therapies must deliver only relevant NO doses for specific durations. In this study, the use of the targeted nanosystem can achieve localized NO delivery to mitochondria, resulting in efficient damage to mitochondria and the amplified level of apoptosis to cancer cells.

Conclusions

In this study, a multifunctional NO-releasing system based on carbon-dot has been fabricated. The intracellular location of the nanosystem can be readily tracked due to the fluorescent nature of the carbon-dot. With mitochondrion-targeting ligands on its surface, the nanosystem can preferentially reside in mitochondrion. The nanosystem displays little dark cytotoxicity at physiological temperature; however, it can damage the mitochondria by releasing NO upon light irradiation, affording a higher cytotoxicity towards cancer cells. We suppose, compared to the previously reported small molecular NO-releasing system,[49,50] this nanosized system may exhibit some advantageous properties such as ease of fabrication (due to the existence of many reaction cites on carbon dot's surface), higher water solubility (no need for using DMSO in cell experiments) and etc.; but it also has inherent drawbacks such as relatively ill-defined structure. This strategy may provide useful insights for rational design of NO-related therapies.

Acknowledgements

We gratefully acknowledge the financial support by NSFC (21474031, 21174040 and 21025415), and the National Key Basic Research Program of China (Project No. 2013CB834702).

Notes and references

College of Materials Science and Engineering, State Key Laboratory of Luminescent Materials and Devices, South China University of Technology, 510640, China
E-mail: mcfzeng@scut.edu.cn, shzhwu@scut.edu.cn

† Electronic Supplementary Information (ESI) available. See DOI: 10.1039/b000000x/

1. A. W. Carpenter and M. H. Schoenfisch, *Chem. Soc. Rev.*, 2012, **41**, 3742.
2. S. Moncada, R. Palmer and E. Higgs, *Pharmacol. Rev.*, 1991, **43**, 109.
3. R. M. Palmer, D. Ashton and S. Moncada, *Nature*, 1988, **333**, 664.
4. V. Calabrese, C. Mancuso, M. Calvani, E. Rizzarelli, D. A. Butterfield and A. M. G. Stella, *Nat. Rev. Neurosci.*, 2007, **8**, 766.
5. A. W. Carpenter and M. H. Schoenfisch, *Chem. Soc. Rev.*, 2012, **41**, 3742.
6. D. Fukumura, S. Kashiwagi and R. K. Jain, *Nat. Rev. Cancer*, 2006, **6**, 521.
7. Z. Liu, W. Li, F. Wang, C. Sun, L. Wang, J. Wang and F. Sun, *Nanoscale*, 2012, **4**, 7135.
8. J. M. Brown and W. R. Wilson, *Nat. Rev. Cancer*, 2004, **4**, 437.
9. X. Wang, K. Liu, G. Yang, L. Cheng, L. He, Y. Liu, Y. Li, L. Guo and Z. Liu, *Nanoscale*, 2014, **6**, 9198.
10. J. Xu, F. Zeng, H. Wu, C. Hu and S. Wu, *Biomacromolecules*, 2014, **15**, 4249.
11. P. G. Wang, M. Xian, X. Tang, X. Wu, Z. Wen, T. Cai and A. J. Janczuk, *Chem. Rev.*, 2002, **102**, 1091.
12. X. Zhang, S. Mansouri, D. Mbeh, L. H. Yahia, E. Sacher and T. Veres, *Langmuir*, 2012, **28**, 12879.
13. A. W. Carpenter, D. L. Slomberg, K. S. Rao and M. H. Schoenfisch, *ACS Nano*, 2011, **5**, 7235.
14. E. V. Stevens, A. W. Carpenter, J. H. Shin, J. Liu, C. J. Der and M. H. Schoenfisch, *Mol. Pharm.*, 2010, **7**, 775.
15. D. A. Riccio, J. L. Nugent and M. H. Schoenfisch, *Chem. Mater.*, 2011, **23**, 1727.
16. P. T. Burks, J. V. Garcia, R. J. GonzalezIrias, J. T. Tillman, M. Niu, A. A. Mikhailovsky, J. Zhang, F. Zhang and P. C. Ford, *J. Am. Chem. Soc.*, 2013, **135**, 18145.
17. A. D. Ostrowski, B. F. Lin, M. V. Tirrell and P. C. Ford, *Mol. Pharm.*, 2012, **9**, 2950.
18. D. Neuman, A. D. Ostrowski, R. O. Absalonson, G. F. Strouse and P. C. Ford, *J. Am. Chem. Soc.*, 2007, **129**, 4146.
19. G. A. Blaise, D. Gauvin, M. Gangal and S. Authier, *Toxicology*, 2005, **208**, 177.
20. E. Deniz, N. Kandoth, A. Fraix, V. Cardile, A. C. Graziano, D. Lo Furno, R. Gref, F. M. Raymo and S. Sortino, *Chem.-Eur. J.*, 2012, **18**, 15782.
21. N. Kandoth, J. Mosinger, R. Gref and S. Sortino, *J. Mater. Chem. B*, 2013, **1**, 3458.
22. S. Sortino, *J. Mater. Chem.*, 2012, **22**, 301.

Journal Name View Article Online DOI: 10.1039/C5TB00522A ARTICLE

23. S. Swaminathan, J. Garcia-Amoros, A. Fraix, N. Kandoth, S. Sortino and F. M. Raymo, *Chem. Soc. Rev.*, 2014, **43**, 4167.
24. P. Taladriz-Blanco, J. Perez-Juste, N. Kandoth, P. Herves and S. Sortino, *J. Colloid Interf. Sci.*, 2013, **407**, 524.
25. G. C. Brown and V. Borutaite, *Free Radic. Biol. Med.*, 2002, **33**, 1440.
26. P. N. Coneski and M. H. Schoenfisch, *Chem. Soc. Rev.*, 2012, **41**, 3753.
27. J. Coulter, H. McCarthy, J. Xiang, W. Roedl, E. Wagner, T. Robson and D. Hirst, *Nitric Oxide*, 2008, **19**, 192.
28. D. A. Riccio and M. H. Schoenfisch, *Chem. Soc. Rev.*, 2012, **41**, 3731.
29. A. B. Seabra and N. Durán, *J. Mater. Chem.*, 2010, **20**, 1624.
30. A. Battigelli, J. Russier, E. Venturelli, C. Fabbro, V. Petronilli, P. Bernardi, T. Da Ros, M. Prato and A. Bianco, *Nanoscale*, 2013, **5,** 9110.
31. W.-H. Chen, G.-F. Luo, X.-D. Xu, H.-Z. Jia, Q. Lei, K. Han and X.-Z. Zhang, *Nanoscale*, 2014, **6**, 9531.
32. S. Fulda, L. Galluzzi and G. Kroemer, *Nat. Rev. Drug Discov.*, 2010, **9**, 447.
33. E. G. Ju, Z. H. Li, Z. Liu, J. S. Ren, X. G. Qu, *ACS Appl. Mater. Interfaces*, 2014, **6**, 4364.
34. K. Han, Y. Liu, W. N. Yin, S. B. Wang, Q. Xu, R. X. Zhuo and X. Z. Zhang, *Adv Healthc Mater*, 2014, DOI: 10.1002/adhm.201400020.
35. W. H. Chen, X. D. Xu, G. F. Luo, H. Z. Jia, Q. Lei, S. X. Cheng, R. X. Zhuo and X. Z. Zhang, *Sci Rep*, 2013, **3**, 3468.
36. R. A. Smith, C. M. Porteous, A. M. Gane and M. P. Murphy, *Proc. Natl. Acad. Sci.*, 2003, **100**, 5407.
37. B. C. Dickinson and C. J. Chang, *J. Am. Chem. Soc.*, 2008, **130**, 9638.
38. S. Marrache and S. Dhar, *Proc. Natl. Acad. Sci.*, 2012, **109**, 16288.
39. S. Marrache, R. K. Pathak and S. Dhar, *Proc. Natl. Acad. Sci.*, 2014, **111**, 10444.
40. L. Boscá and S. Hortelano, *Cell. Signal.*, 1999, 11, 239.
41. C. Giulivi, J. J. Poderoso and A. Boveris, *J. Biol. Chem.*, 1998, 273, 11038.
42. A. J. Hobbs, A. Higgs and S. Moncada, *Annu. Rev. Pharmacol. Toxicol.*, 1999, **39**, 191.
43. H. O. McCarthy, J. A. Coulter, T. Robson and D. G. Hirst, *J. Pharm. Pharmacol.*, 2008, **60**, 999.
44. E. Nisoli, E. Clementi, C. Paolucci, V. Cozzi, C. Tonello, C. Sciorati, R. Bracale, A. Valerio, M. Francolini and S. Moncada, *Science*, 2003, **299**, 896.
45. S. Shiva, J.-Y. Oh, A. L. Landar, E. Ulasova, A. Venkatraman, S. M. Bailey and V. M. Darley-Usmar, *Free Radical Biology and Medicine*, 2005, **38**, 297.
46. R. Scatena, in *Advances in Mitochondrial Medicine*, Springer, 2012, pp. 329.
47. S. Kumar, W.-K. Rhim, D.-K. Lim and J.-M. Nam, *ACS Nano*, 2013, **7**, 2221.
48. N. A. Belikova, J. Jiang, D. A. Stoyanovsky, A. Glumac, H. Bayir, J. S. Greenberger and V. E. Kagan, *FEBS Lett.*, 2009, **583**, 1945.
49. T. Horinouchi, H. Nakagawa, T. Suzuki, K. Fukuhara and N. Miyata, *Bioorg. Med. Chem. Lett.*, 2011, **21**, 2000
50. T. Horinouchi, H. Nakagawa, T. Suzuki, K. Fukuhara and N. Miyata, *Chem. Eur. J.*, 2011, **17**, 4809.
51. J. Xu, F. Zeng, H. Wu, C. Hu, C. Yu and S. Wu, *Small*, 2014,**10**, 3750
52. X. H. Wang, K. G. Qu, B. L. Xu, J. S. Ren and X. G. Qu, *J. Mater. Chem.*, 2011, **21**, 2445.
53. H. Liu, Q. Wang, G. Shen, C. Zhang, C. Li, W. Ji, C. Wang and D. Cui, *Nanoscale Res. Lett.*,2014, 9, 397.
54. Y. C. Song, W. Shi, W. Chen, X. H. Li and H. M. Ma, *J. Mater. Chem.*, 2012, **22**, 12569.
55. G. S. Tong, J. X. Wang, R. B. Wang, X. Q. Guo, L. He, F. Qiu,G. Wang, B. S. Zhu, X. Y. Zhu and T. Liu, *J. Mater. Chem.B*, 2015, **3**, 700.
56. G. F. Wu, F. Zeng, C. M. Yu, S. Z. Wu and W. S. Li, *J. Mater. Chem. B*, 2014, **2**, 8528.
57. P. Huang, J. Lin, X. Wang, Z. Wang, C. Zhang, M. He, K. Wang, F. Chen, Z. Li, G. Shen, D. Cui and X. Chen, *Adv. Mater.*, 2012, **24**, 5104.
58. T. B. Cai, D. Lu, M. Landerholm and P. G. Wang, *Org. Lett.*, 2004, **6**, 4203.
59. S. Mocellin, V. Bronte and D. Nitti, *Med. Res. Rev.*, 2007, 27, 317.
60. J. M. Adams, *Genes Dev.*, 2003, **17**, 2481.
61. J. Ly, D. Grubb and A. Lawen, *Apoptosis*, 2003, **8**, 115.
62. D. Chaoui, A. M. Faussat, P. Majdak, R. Tang, J. Y. Perrot, S. Pasco, C. Klein, J. P. Marie and O. Legrand, *Cytom. Part B: Clin. Cy.*, 2006, 70, 189.

View Article Online
DOI: 10.1039/C5TB00522A

A spatiotemporally controllable NO-releasing nanosystem for killing cancer cells with high efficiency based on carbon dots has been developed, which exhibits mitochondria targeting, light-responsive NO-releasing and cell imaging capability.